Heliyon 10 (2024) e37264

Contents lists available at ScienceDirect

Heliyon

journal homepage: www.cell.com/heliyon

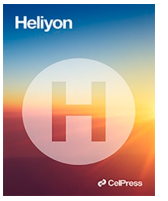

Research article

# Hsa_circ_0000825 promotes the progression of laryngeal squamous cell carcinoma by sponging miR-766 and interacting with ELAVL1

Miaomiao Yu, Huan Cao, Jianwang Yang, Tao Liu, Baoshan Wang *

*Department of Otorhinolaryngology, The Second Hospital of Hebei Medical University, Shijiazhuang, China*

ARTICLE INFO

*Keywords:*
Laryngeal squamous cell carcinoma
hsa_circ_0000825
miR-766
HOXD10
ELAVL1

ABSTRACT

Emerging evidence suggests that circular RNAs (circRNAs) are involved in the regulation of tumourigenesis and progression of a variety of malignant tumours. In this study, we aimed to identify laryngeal squamous cell carcinoma (LSCC)-specific circRNAs and explore their biological functions and underlying molecular mechanisms. Employing microarray and qRT-PCR, hsa_circ_0000825 was found to be significantly increased in LSCC tissues versus para-cancerous tissues. High hsa_circ_0000825 expression was positively associated with advanced clinical stages, lymph node metastasis, and poor survival. Furthermore, the overexpression of hsa_circ_0000825 in TU177 and AMC-HN-8 cells promoted cell proliferation. Transwell assays showed enhanced migration and invasion of TU177 and AMC-HN-8 cells upon overexpression of hsa_circ_0000825. Conversely, the knockdown of hsa_circ_0000825 had the opposite effect. Xenograft tumours in BALB/c nude mice derived from hsa_circ_0000825-overexpressed TU177 cells showed greater volume and weight than those derived from control TU177 cells. Mechanistically, nuclear-cytoplasmic fractionation assay confirmed that hsa_circ_0000825 was mainly located in the cytoplasm of TU177 and AMC-HN-8 cells. The AGO2-RNA immunoprecipitation (RIP) assay revealed that hsa_circ_0000825 was significantly enriched in the AGO2-precipitated complex in both TU177 and AMC-HN-8 cells, suggesting that this circRNA may function via a competitive endogenous RNA (ceRNA) mechanism. Next, bioinformatics analysis, biotinylated-oligo pull-down assay and dual-luciferase reporter assay verified that miR-766 could be sponged by hsa_circ_0000825 and also target 3′UTR of HOXD10 mRNA. Moreover, miR-766 was shown to be involved in the pro-oncogenic effect of hsa_circ_0000825. This occurred via the mediation of hsa_circ_0000825-enhanced HOXD10 mRNA by the ceRNA mechanism in TU177 and AMC-HN-8 cells. Besides, RNA-binding protein (RBP) ELAVL1 interacted with hsa_circ_0000825 in TU177 and AMC-HN-8 cells, as revealed through bioinformatics analysis, biotinylated-oligo pull-down assays, and RIP assays. ELAVL1 knockdown decreased cell proliferation by 38 % and 34 % in hsa_circ_0000825-overexpressed TU177 and AMC-HN-8 cells ($P < 0.05$). Similarly, ELAVL1 was involved in the pro-migration and pro-invasion effects of hsa_circ_0000825 overexpression. In addition, comprehensive analysis of mRNA-seq in hsa_circ_0000825-overexpressed TU177 cells, as well as catRAPID and TCGA databases, suggested that ITGB2, HOXD10, and MTCL1 might be crucial downstream target mRNAs of ELAVL1 in LSCC, participating in the hsa_circ_0000825-ELAVL1 axis pro-oncogenic effect. Taken together, hsa_circ_0000825 plays a pro-oncogenic role

* Corresponding author. Department of Otorhinolaryngology, The Second Hospital of Hebei Medical University, 215 Heping West Road, Shijiazhuang, 050000, China.
*E-mail address:* wangbaoshan@hebmu.edu.cn (B. Wang).

https://doi.org/10.1016/j.heliyon.2024.e37264
Received 23 June 2024; Received in revised form 16 August 2024; Accepted 29 August 2024
Available online 1 September 2024

in LSCC via the miR-766/HOXD10 axis and ELAVL1 and may serve as a promising specific biomarker and therapeutic target for LSCC.

## 1. Introduction

Laryngeal squamous cell carcinoma (LSCC) is a common type of squamous cell carcinoma of the head and neck, accounting for approximately 25–30 % of cases [1]. In 2020, there were 184,615 diagnosed cases of LSCC worldwide, with 99,840 deaths [2]. The onset of LSCC is insidious, with early symptoms often vague and non-specific, leading many patients to be diagnosed at advanced stages (clinical stages III and IV) [3]. Owing to the anatomical limitations of the throat and abundant submucosal lymph nodes, LSCC is prone to local invasion and cervical lymph node metastasis [4]. Currently, surgery, radiotherapy, and chemotherapy are the primary treatment methods for LSCC, but targeted therapy is very limited [5]. According to data from the Surveillance, Epidemiology, and End Results Program, the 5-year relative survival rate of patients with laryngeal cancer was estimated to be 61.6 % from 2013 to 2019 [6]. Therefore, it is crucial to explore the pathological mechanisms involved in the occurrence and development of LSCC and to search for potential specific biomarkers and therapeutic targets.

Circular RNAs (circRNAs) are non-coding RNA molecules that have covalently closed loop structures without a 5′ cap and 3′ poly(A) tail [7]. With the continuous progress in biological technologies, an increasing number of circRNAs have been identified through RNA sequencing, and their characteristics, such as stability, sequence conservation, and expression specificity, have been revealed [8]. CircRNAs are also involved in the regulation of tumourigenesis and progression of a variety of malignant tumours [9]. The mechanisms by which circRNAs affect cell function include acting as sponges for microRNAs (miRNAs), competing with mRNAs for binding to RNA-binding proteins (RBPs), interacting with proteins to influence their stability and function, binding to RNA polymerase II to regulate gene transcription, and encoding polypeptides, etc. [10–14] Because of their stability, disease specificity, and function, circRNAs are ideal candidates for the early diagnosis, prognosis evaluation, and treatment of malignant tumours [9]. Therefore, studying the expression, function, and molecular mechanisms of circRNAs in LSCC is very important for the discovery and identification of specific biomarkers and ideal therapeutic targets.

In the present study, hsa_circ_0000825 expression was significantly higher in LSCC tissues than in para-cancerous tissues. High hsa_circ_0000825 expression was positively associated with advanced clinical stages, lymph node metastasis, and poor survival. Furthermore, hsa_circ_0000825 overexpression promoted the proliferation, migration, and invasion of TU177 and AMC-HN-8 cells *in vitro* and the growth of TU177 cell-derived xenograft tumours *in vivo*. Mechanistically, miR-766 could be sponged by hsa_circ_0000825, and also target 3' untranslated region (3′UTR) of HOXD10 mRNA. Moreover, miR-766 was involved in the pro-oncogenic effect of hsa_circ_0000825 by mediating hsa_circ_0000825-enhanced HOXD10 mRNA through ceRNA mechanism in TU177 and AMC-HN-8 cells. Besides, the RBP ELAVL1 interacted with hsa_circ_0000825 in TU177 and AMC-HN-8 cells. Then, knockdown of ELAVL1 attenuated the pro-proliferation, pro-migration, and pro-invasion effects of hsa_circ_0000825 overexpression in TU177 and AMC-HN-8 cells. In addition, comprehensive analysis of mRNA-seq in hsa_circ_0000825-overexpressed TU177 cells, as well as catRAPID and TCGA databases, indicated that ITGB2, HOXD10, and MTCL1 may be crucial downstream target mRNAs of ELAVL1 in LSCC, participating in the hsa_circ_0000825-ELAVL1 axis pro-oncogenic effect.

## 2. Materials and methods

### 2.1. LSCC patient tissues

Forty-eight pairs of LSCC and matched para-cancerous tissues were collected from surgical patients at The Second Hospital of Hebei Medical University. None of the patients received radiotherapy or chemotherapy before surgery. This study was approved by the Medical Ethics Committee of Hebei Medical University (P2022067, March 10, 2022). All enrolled patients provided written informed consent.

### 2.2. Cell lines and cell culture

Human LSCC cell lines (TU177 and AMC-HN-8), human nasopharyngeal epithelial cell line (NP69), and HEK293T cell line were used in this study. All the cell lines were stored in the Biobank of Otorhinolaryngology Head and Neck Surgery of Hebei Medical University. TU177 cells were grown in RPMI1640 medium (Gibco, Shanghai, China) containing 10 % fetal bovine serum (FBS) (Lonsera, Uruguay). AMC-HN-8 and HEK293T cells were maintained in DMEM medium (Gibco, Shanghai, China) containing 10 % FBS. NP69 cells were grown in keratinocyte medium (ScienCell, United States) containing 1 % keratinocyte growth supplement (ScienCell, United States) and 1 % penicillin/streptomycin solution (ScienCell, United States). All cells were cultured in an incubator at 37 °C with 5 % $CO_2$.

### 2.3. RNA extraction, genomic DNA (gDNA) extraction, and qRT-PCR

Total RNA was extracted from tissues and cells using the RNA-easy Isolation Reagent (Vazyme, Nanjing, China) according to the manufacturer's instructions. The PARIS™ Kit (Invitrogen, California, USA) was utilised to isolate nuclear and cytoplasmic RNA

fractions. Genomic DNA was isolated with a DNA Extraction Reagent (Solarbio, Beijing, China). Transcriptor First Strand cDNA Synthesis Kit (Roche Diagnosis, Mannheim, Germany) was used for reverse transcription. Sequences of the stem-loop RT primers for the miRNAs are listed in Supplemental Table 1 qRT-PCR was conducted according to the instruction of GoTaq®qPCR Master Mix (Promega, Wisconsin, USA). GAPDH or 18S rRNA was used as an internal control for circRNA and mRNA, while miRNA expression was normalised by U6. The fold change was expressed in the $2^{-\Delta\Delta Ct}$ method. Sequences of the PCR primers are listed in Supplemental Table 1.

### 2.4. Sanger sequencing

Sanger sequencing was conducted by Sangon Biotech (Shanghai, China) to confirm the amplification products of circRNAs.

### 2.5. RNase R treatment

RNase R (3U/μg, Epicentre Technologies, Wisconsin, USA) was added to total RNA (2 μg) of LSCC cells in the experimental groups, while solvent was added to the control group. The mixture was incubated at 37 °C for 25 min and 70 °C for 10 min, according to the manufacturer's instructions. RT-PCR was conducted to analyse the products.

### 2.6. Cell transfection

The hsa_circ_0000825 overexpression plasmid was purchased from HanBio (Shanghai, China). HOXD10 and ELAVL1 overexpression plasmid were purchased from YouBio (Changsha, China). To knockdown hsa_circ_0000825, HOXD10, and ELAVL1, the DNA oligo of the corresponding short hairpin RNA was cloned into the pGenesil-1 vector (YouBio, Changsha, China). For luciferase reporter plasmids, the hsa_circ_0000825 sequence and HOXD10 3′UTR sequence of wild type or miR-766 binding site mutant were cloned into the pmirGLO vector (YouBio, Changsha, China). MiR-766 mimics and inhibitor were synthesised by RiboBio (Guangzhou, China). Lipofectamine 2000 (Invitrogen, California, USA) was used for transient transfection of cells according to the manufacturer's instructions. The sequences used for plasmid construction and the miR-766 mimics and inhibitor sequences are listed in Supplemental Table 1.

### 2.7. MTS assay

CellTiter 96® AQueous One Solution Cell Proliferation Assay Kit (Promega, Wisconsin, USA) was used to detect the proliferation ability of transfected LSCC cells. Cells ($2 \times 10^3$ cells per well) were seeded in 96-well plate, and 20 μl MTS was added into each well. The cells were incubated at 37 °C for 2 h. The absorbance was measured at 490 nm wavelength using a microplate reader (Mod: SPARK 10 M, TECAN, Switzerland).

### 2.8. Colony formation assay

A total of $2 \times 10^3$ LSCC cells were collected and seeded into a 6-well plate, followed by culturing at 37 °C for 10 days. After removing the culture medium, the cells were fixed with 4 % paraformaldehyde for 20 min and stained with 0.1 % crystal violet for 20 min. The number of colonies was then counted.

### 2.9. Transwell migration and invasion assays

A total of $1 \times 10^5$ LSCC cells transfected for 48 h were suspended in 100–200 μl of serum-free medium. The cell suspension was then added to the upper chamber of the transwell chamber (Corning, New York, USA) and medium (650 μl) containing 10 % FBS was placed in the lower chamber. The invasion assay was conducted using transwell chambers pre-coated with Matrigel (Corning, New York, USA). After 24 h of routine incubation, cells that did not thread through the filter membrane were removed, and cells that threaded through the filter membrane were fixed with 4 % paraformaldehyde for 20 min and stained with 0.1 % crystal violet for 20 min. Finally, the cells were counted under a microscope.

### 2.10. RNA immunoprecipitation (RIP)

RIP assay was used to verify the binding between AGO2 and hsa_circ_0000825 and between ELAVL1 and hsa_circ_0000825. According to the instructions of the RNA Immunoprecipitation Kit (Geneseed Biotech, Guangzhou, China), $1 \times 10^7$ cells were collected, and 1 ml lysis buffer containing protease inhibitors and RNase inhibitors was added to the cells. The protein A + G magnetic beads combined with AGO2 antibody (#ab186733; Abcam, Cambridge, USA), FLAG antibody (#0912–1; HUABIO, Hangzhou, China), or IgG (# HA1002; HUABIO, Hangzhou, China) were added to the cell lysate and incubated overnight at 4 °C. Proteins and RNA were collected separately. Western blot analysis was conducted to verify the validity of the experiment, and qRT-PCR was used to verify the enrichment of hsa_circ_0000825.

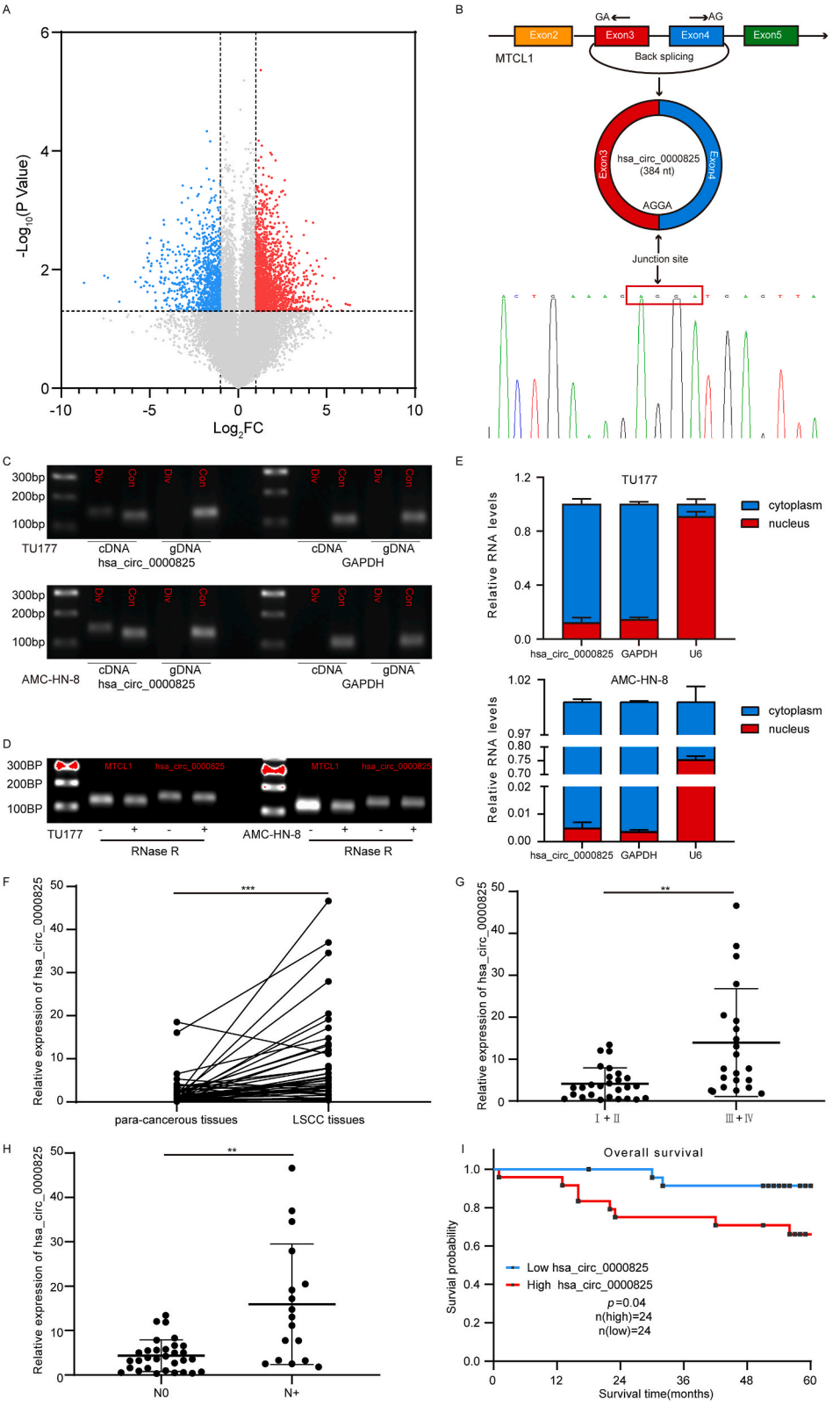


*(caption on next page)*

**Fig. 1.** Identification, characteristics, expression and clinical significance of hsa_circ_0000825 in LSCC
**A** Volcano plot of the differentially expressed circRNAs in three pairs of LSCC tissues and para-cancerous tissues. The red dots represent higher expression levels, while the blue dots represent lower expression levels. **B** Schematic illustration showed the cyclization of MTCL1 exons 3 and 4 to form hsa_circ_0000825. Sanger sequencing following RT-PCR was used to show the "head-to-tail" splicing of hsa_circ_0000825. **C** Hsa_circ_0000825 expression in LSCC cells verified by RT-PCR. Agarose gel electrophoresis showed that divergent primers amplified hsa_circ_0000825 in cDNA but not in gDNA. GAPDH served as a negative control. **D** Validation of hsa_circ_0000825 stability by RNase R treatment and RT-PCR assay. **E** Hsa_circ_0000825 abundance in nuclear and cytoplasmic fractions of LSCC cells was evaluated by qRT-PCR. GAPDH acted as a positive control of RNA distributed in the cytoplasm, and U6 RNA acted as a positive control of RNA distributed in the nucleus. **F** Expression levels of hsa_circ_0000825 in 48 paired LSCC tissues were determined by qRT-PCR. **G-H** The expression of hsa_circ_0000825 in different groups was evaluated according to the clinical features ($n_{\text{(clinical stage I+II)}} = 27$, $n_{\text{(clinical stage III+IV)}} = 21$; $n_{(N0)} = 31$, $n_{(N+)} = 17$). **I** Kaplan-Meier analysis of the correlation between hsa_circ_0000825 expression and overall survival. $^{*}P < 0.05$, $^{**}P < 0.01$, $^{***}P < 0.001$. Div, divergent primer; Con, convergent primer; N0, patients without cervical lymph node metastasis; N+, patients with cervical lymph node metastasis.

### 2.11. Biotinylated-oligo pull-down assay

Biotinylated-oligo pull-down assay was performed to detect the miRNAs and RBPs that could bind to hsa_circ_0000825. Briefly, $4 \times 10^7$ cells were cross-linked with formaldehyde, and the cross-linking was then quenched with glycine. Subsequently, the cells were lysed and incubated with biotinylated-oligo probes (RiboBio Shanghai, China) for 4h at 37 °C. Next, the probes-lysate complex was captured using streptavidin beads. RNA and proteins were collected separately. qRT-PCR was used to analyse the miRNAs binding to hsa_circ_0000825. Western blot analysis was performed to analyse the RBP of hsa_circ_0000825. The probe sequences are listed in Supplemental Table 1.

### 2.12. Dual-luciferase reporter assay

MiR-766 mimics or NC mimics and luciferase reporter plasmids were co-transfected into HEK293T cells. Cells transfected for 48 h were lysed, and luciferase activity was measured according to the instructions of the Dual-Luciferase Reporter Assay System (Promega, Wisconsin, USA). The ratio of firefly luciferase to renilla luciferase activity was used to represent relative luciferase activity.

### 2.13. Western blot analysis

Total protein was extracted using RIPA lysis buffer (Solarbio, Beijing, China) containing protease inhibitor cocktail (Promega, Wisconsin, USA). The BCA Protein Assay Kit (Generay, Shanghai, China) was used to determine the protein concentration. Protein (20μg/sample) was separated via SDS-PAGE and transferred onto polyvinylidene difluoride (PVDF) membranes (Bio-Rad, California, USA). The PVDF membranes were blocked with 5 % skim milk (Biofroxx, Einhausen, Germany) for 2 h at room temperature and incubated with primary antibodies against AGO2 (#ab186733, 1:2000; Abcam, Cambridge, USA), HOXD10 (#sc-166235, 1:1000; Santa Cruz, Shanghai, China), ELAVL1 (#1862775, 1:1000; Thermo Scientific, Shanghai, China), FLAG (#0912–1, 1:5000; HUABIO, Hangzhou, China), β-Actin (#66009-1-Ig, 1:20000; Proteintech, Wuhan, China), or β-Tublin (#10094-1-AP, 1:10000; Proteintech, Wuhan, China) overnight at 4 °C. After washing three times with TBST, the membranes were incubated with secondary antibodies for 2 h at room temperature. The bands were visualised using enhanced chemiluminescence (ECL) detection reagents (Vazyme, Nanjing, China) with ChemiDoc™ XRS + System (Bio-Rad, California, USA).

### 2.14. Generation of hsa_circ_0000825 overexpression cells and xenograft tumorigenesis

The hsa_circ_0000825 overexpression lentivirus was purchased from HanBio (Shanghai, China). The viral supernatant was added to TU177 cells and incubated for 72 h. Puromycin (2 μg/ml) was then added and incubated for 48 h, and the stable cells were screened. Male SPF-grade BALB/c nude mice (5–6 weeks) were purchased from Beijing Vital River Laboratory Animal Technology Co., Limited. (Beijing, China). The mice were randomly divided into two groups, with seven mice per group. Cells were collected and resuspended in PBS, and $5 \times 10^6$ cells (200 μl) were subcutaneously injected into each mouse. The tumour volume was measured every 7 days after injection. After 28 days, the mice were euthanised, and the tumours were weighed. Tumour volume was calculated using the following formula: V (volume) = (length × width$^2$)/2. The animal experiments in this study were approved by the Laboratory Animal Ethical and Welfare Committee of Hebei Medical University (LACUC-Hebmu-P 2022101, March 11, 2022).

### 2.15. Statistical analysis

SPSS 25.0 and GraphPad Prism 9 were used for statistical analysis. Differences between the two groups were assessed using a two-tailed Student's t-test or Mann-Whitney *U* test. Kaplan-Meier survival curve and log-rank test were used to compare overall survival. Data are presented as mean ± standard deviation (SD). *P* values of $<0.05$ was set as the threshold for significant difference.

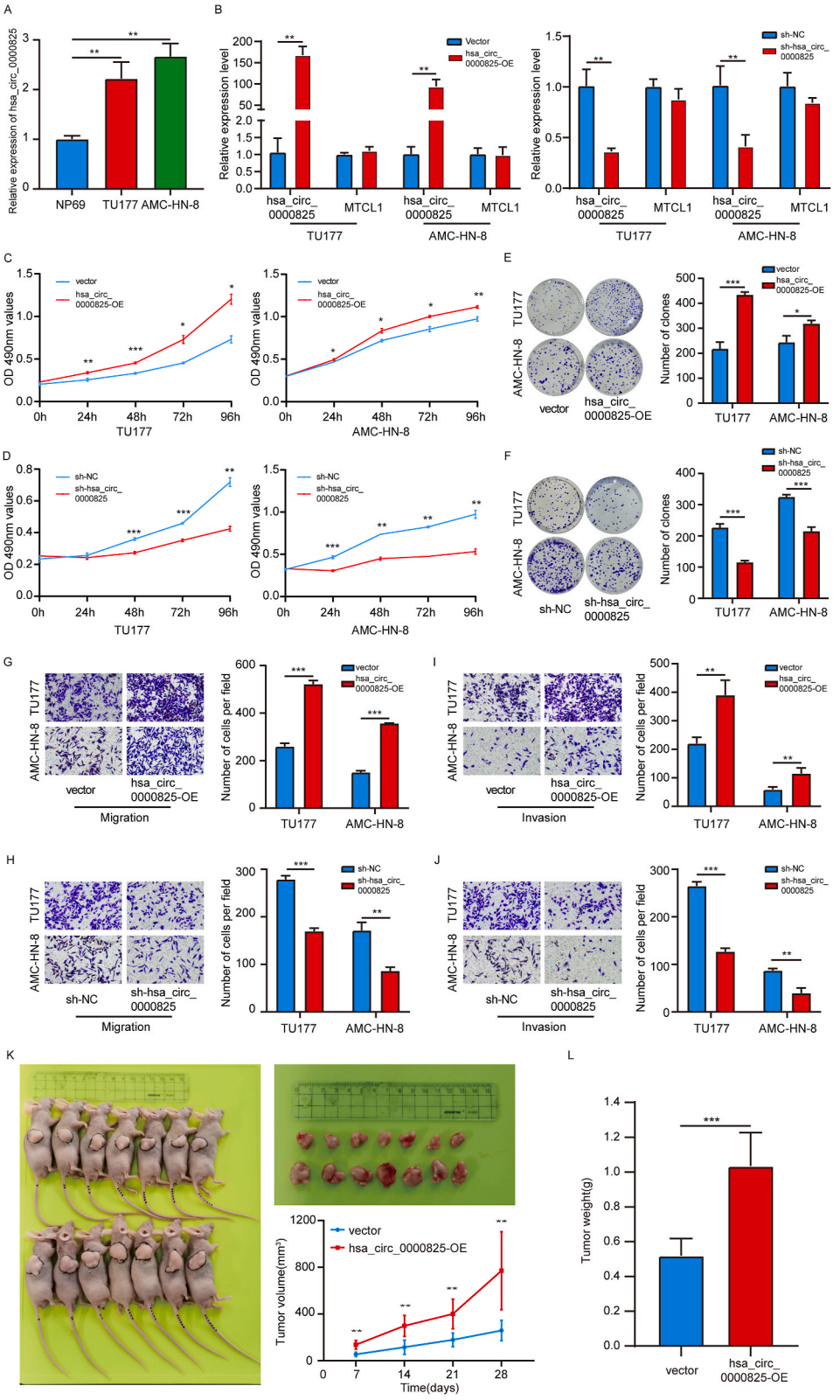


*(caption on next page)*

**Fig. 2.** Hsa_circ_0000825 promoted proliferation, migration and invasion of LSCC cells *in vitro* and the growth of tumours derived from TU177 cells *in vivo*

**A** qRT-PCR analysis of the hsa_circ_0000825 expression in human LSCC cell lines (TU177 and AMC-HN-8) and human nasopharyngeal epithelial cell line (NP69). **B** The efficacy of hsa_circ_0000825 overexpression plasmid and knockdown plasmid were detected by qRT-PCR. **C&D** The effect of hsa_circ_0000825 on cell vitality in TU177 and AMC-HN-8 cells was detected by MTS assay. **E&F** Up-regulation of hsa_circ_0000825 prominently promoted the colony formation of LSCC cells, while the colony formation of LSCC cells in hsa_circ_0000825 down-regulated group was repressed. **G-J** The cell migration and invasion ability of LSCC cells after overexpression and knockdown of hsa_circ_0000825 were examined by transwell assay. **K** Images of xenograft tumours in nude mice. And comparison of the tumor volume in hsa_circ_0000825-OE and control group (n = 7 each group). **L** Comparison of the tumor weight in hsa_circ_0000825-OE and control group (n = 7 each group). $^{*}P < 0.05$, $^{**}P < 0.01$, $^{***}P < 0.001$.

## 3. Results

### 3.1. Identification and characteristics of hsa_circ_0000825 in LSCC

Three pairs of LSCC and para-cancerous tissues were selected for transcriptome microarray analysis to identify LSCC-specific circRNAs. There were 3256 significantly differentially expressed ($|\log_2 FC| \geq 1$ and $P < 0.05$) circRNAs, including 2159 upregulated circRNAs and 1097 downregulated circRNAs (Fig. 1A). Among these, hsa_circ_0000825 ($\log_2 FC = 1.73$ and $P = 0.017$) was significantly increased in LSCC tissues. As reported for circBase, hsa_circ_0000825 (chr18:8718421–8720494) is composed of head-to-tail splicing of exon 3–4 (384bp) of MTCL1 gene. Next, through Sanger sequencing, we confirmed that the back-splice site sequence of hsa_circ_0000825 was 'AGGA' in TU177 cells (Fig. 1B). Furthermore, cDNA and gDNA were amplified using divergent and convergent primers. Hsa_circ_0000825 could be amplified by divergent primers in cDNA rather than in gDNA of TU177 and AMC-HN-8 cells. Linear MTCL1 could be amplified by convergent primers in both cDNA and gDNA (Fig. 1C). To confirm the circular structure of hsa_circ_0000825 in TU177 and AMC-HN-8 cells, we performed RNase R digestion experiments. As seen in Fig. 1D, the linear MTCL1 was mostly degraded after RNase R digestion. Differentially, the circular hsa_circ_0000825 expression was not significantly altered by RNase R digestion. Subsequently, hsa_circ_0000825 was confirmed to be mainly located in the cytoplasm of TU177 and AMC-HN-8 cells by nuclear-cytoplasmic fractionation assay (Fig. 1E).

### 3.2. Expression of hsa_circ_0000825 in patients with LSCC and its clinical significance

We further used qRT–PCR to detect the expression of hsa_circ_0000825 in 48 pairs of tissue samples, including LSCC tissues and the corresponding para-cancerous tissues. Hsa_circ_0000825 was significantly upregulated in LSCC tissues compared to para-cancerous tissues ($P < 0.001$) (Fig. 1F). Next, we investigated the correlation between hsa_circ_0000825 expression and the clinicopathological features of patients with LSCC. Hsa_circ_0000825 expression was related to clinical stage, lymph node metastasis, and prognosis. In detail, the expression of hsa_circ_0000825 in stages III and IV was significantly higher than that in stages I and II ($P < 0.01$) (Fig. 1G). Patients with cervical lymph node metastasis had higher expression levels of hsa_circ_0000825 than those without cervical lymph node metastasis ($P < 0.01$) (Fig. 1H). In addition, Kaplan-Meier survival analysis showed that patients with high hsa_circ_0000825 expression had poorer overall survival than those with low expression ($P = 0.04$) (Fig. 1I).

### 3.3. Hsa_circ_0000825 promoted proliferation, migration, and invasion of LSCC cells in vitro and the growth of tumours derived from TU177 cells in vivo

We further investigated the expression of hsa_circ_0000825 in human LSCC cell lines (TU177 and AMC-HN-8) and human nasopharyngeal epithelial cell line (NP69). Hsa_circ_0000825 expression was approximately increased by 2.2 times in TU177 cells and nearly 2.7 times in AMC-HN-8 cells compared to that in NP69 cells (Fig. 2A). To elucidate the biological function of hsa_circ_0000825 in LSCC cells, the hsa_circ_0000825 recombinant expression plasmid and shRNA plasmid were transfected into TU177 and AMC-HN-8 cells. As shown by the qRT-PCR results, the transfection successfully upregulated or downregulated hsa_circ_0000825 expression without affecting the expression of linear MTCL1 mRNA (Fig. 2B). The MTS assay revealed that overexpression of hsa_circ_0000825 significantly promoted the viability of TU177 and AMC-HN-8 cells, whereas knockdown of hsa_circ_0000825 markedly inhibited cell viability (Fig. 2C and D). The colony formation assay demonstrated that upregulation of hsa_circ_0000825 increased cell proliferation by approximately 2 times and 1.3 times in TU177 and AMC-HN-8 cells, respectively, whereas the proliferation of TU177 and AMC-HN-8 cells in the hsa_circ_0000825 downregulated group was reduced by approximately 49 % and 34 %, respectively (Fig. 2E and F). We also verified the effects of hsa_circ_0000825 on the migration and invasion of LSCC cells. Transwell assay results showed that the migration of TU177 and AMC-HN-8 cells in the hsa_circ_0000825 upregulated group was enhanced by approximately 2 times and 2.4 times, respectively, while downregulation of hsa_circ_0000825 decreased cell migration by approximately 39 % and 50 % in TU177 and AMC-HN-8 cells, respectively (Fig. 2G and H). Similarly, the invasion of LSCC cells was enhanced by the overexpression of hsa_circ_0000825 and suppressed by the knockdown of hsa_circ_0000825 (Fig. 2I and J). To explore the effect of hsa_circ_0000825 on LSCC growth *in vivo*, we constructed xenograft tumour models in nude mice by subcutaneously injecting TU177 cells that stably overexpressed hsa_circ_0000825 or control cells. The volume and weight of xenograft tumours formed by hsa_circ_0000825 overexpressing TU177 cells were significantly higher than those in the control group (Fig. 2K and L).

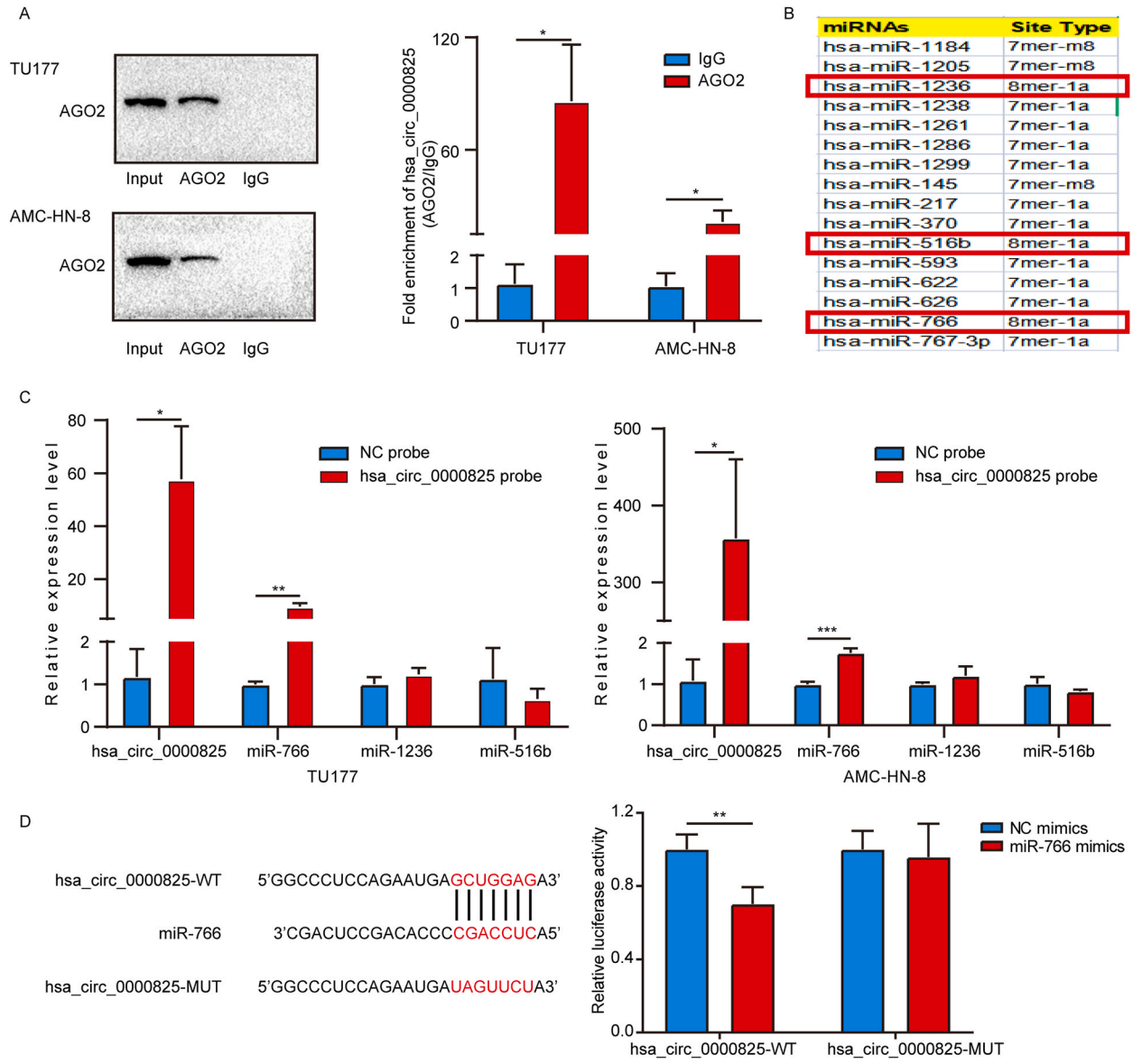


**Fig. 3.** Hsa_circ_0000825 acts as a sponge for miR-766 in LSCC
**A** RIP assay was carried out with AGO2 antibody in TU177 and AMC-HN-8 cells, and then the enrichment of hsa_circ_0000825 was detected by qRT-PCR. **B** The potential-binding miRNAs were predicted by Circular RNA Interactome. **C** Relative level of hsa_circ_0000825 and three miRNAs in TU177 and AMC-HN-8 lysates after RNA pull down using hsa_circ_0000825 probe or NC probe. **D** HEK293T cells were co-transfected with miR-766 mimics and wild-type (hsa_circ_0000825-WT) or mutant (hsa_circ_0000825-MUT) hsa_circ_0000825 luciferase reporter vector, and luciferase activity was detected. $*P < 0.05$, $**P < 0.01$, $***P < 0.001$. NC, negative control.

### *3.4. Hsa_circ_0000825 acts as a sponge for miR-766 in LSCC*

Hsa_circ_0000825 is mainly located in the cytoplasm, therefore, we investigated whether it binds to miRNAs. The AGO2-RIP assay revealed that hsa_circ_0000825 was significantly enriched in the AGO2-precipitated complex compared with the IgG precipitate in both TU177 and AMC-HN-8 cells, suggesting that this circRNA may function through a ceRNA mechanism (Fig. 3A). Next, the potential-binding miRNAs were predicted using the Circular RNA Interactome, in which the miRNAs with the 8mer-1a site type included miR-1236, miR-516b, and miR-766 (Fig. 3B). Furthermore, biotinylated-oligo pull-down assays were conducted in both TU177 and AMC-HN-8 cells, and the results suggested that miR-766, but not miR-1236 or miR-516b, was considerably enriched in the hsa_circ_0000825-specific probe pull-down sample compared to that in the control group (Fig. 3C). Besides, dual-luciferase reporter assay was performed to confirm the direct binding between hsa_circ_0000825 and miR-766. The results revealed that miR-766 mimics diminished the luciferase activity of the hsa_circ_0000825 wild-type reporter gene by approximately 30 % but had no significant effect

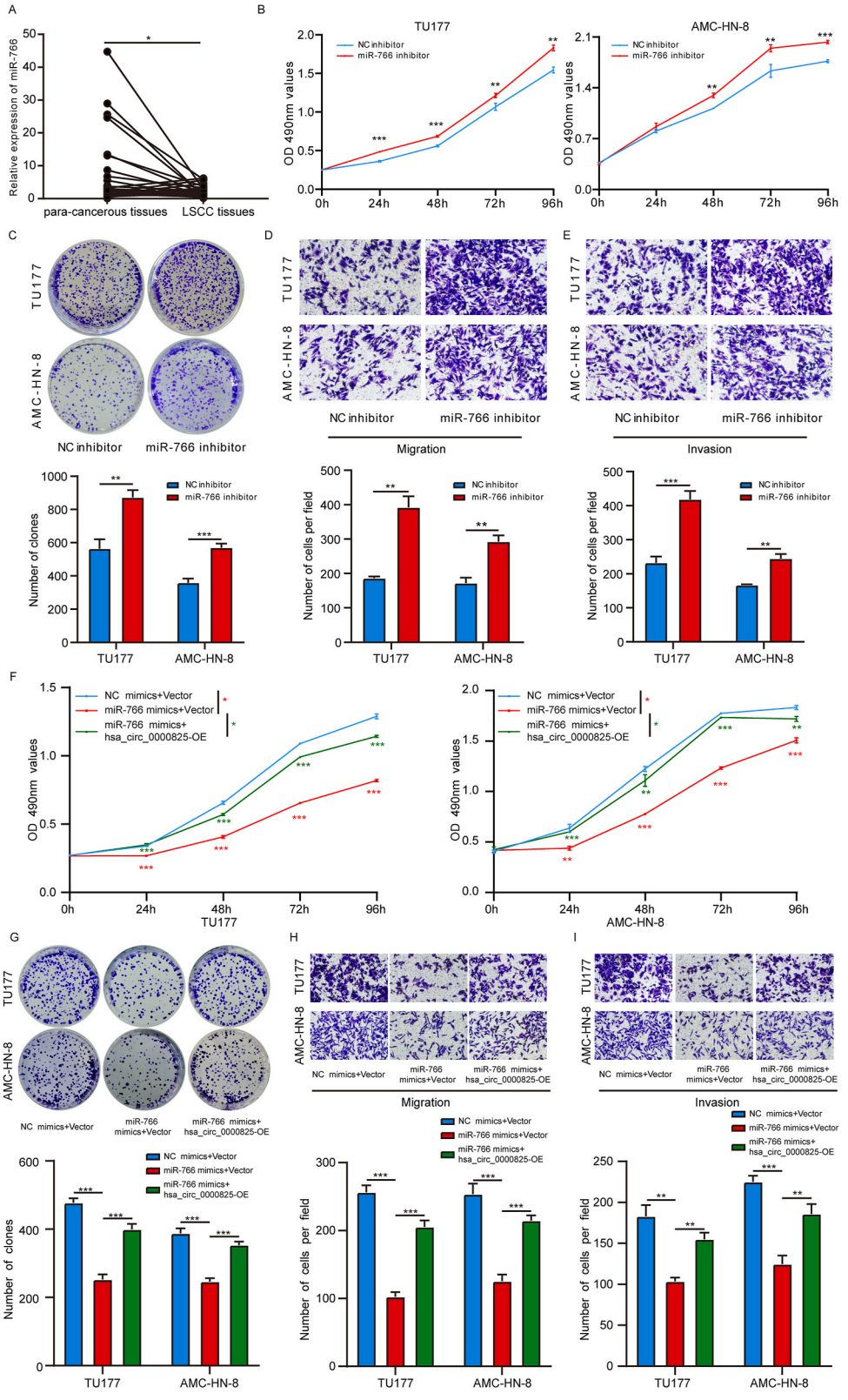


*(caption on next page)*

**Fig. 4.** MiR-766 partially mediate the pro-oncogenic function of hsa_circ_0000825 in LSCC
**A** Expression levels of miR-766 in LSCC tissues were determined by qRT-PCR. **B** The effect of miR-766 on cell vitality in LSCC cells was detected by MTS assay. **C** MiR-766 inhibitor promoted colony formation of both TU177 and AMC-HN-8 cells. **D&E** The cell migration and invasion ability of LSCC cells after miR-766 knockdown were examined by transwell assay. **F&G** MTS and colony formation assays indicated that cell proliferation ability of LSCC cells transfected with miR-766 mimics was partially reversed when co-transfected with overexpression plasmid of hsa_circ_0000825. **H&I** Transwell assay demonstrated that cell migration and invasion abilities of LSCC cells transfected with miR-766 mimics were attenuated when co-transfected with overexpression plasmid of hsa_circ_0000825. $^{*}P < 0.05$, $^{**}P < 0.01$, $^{***}P < 0.001$.

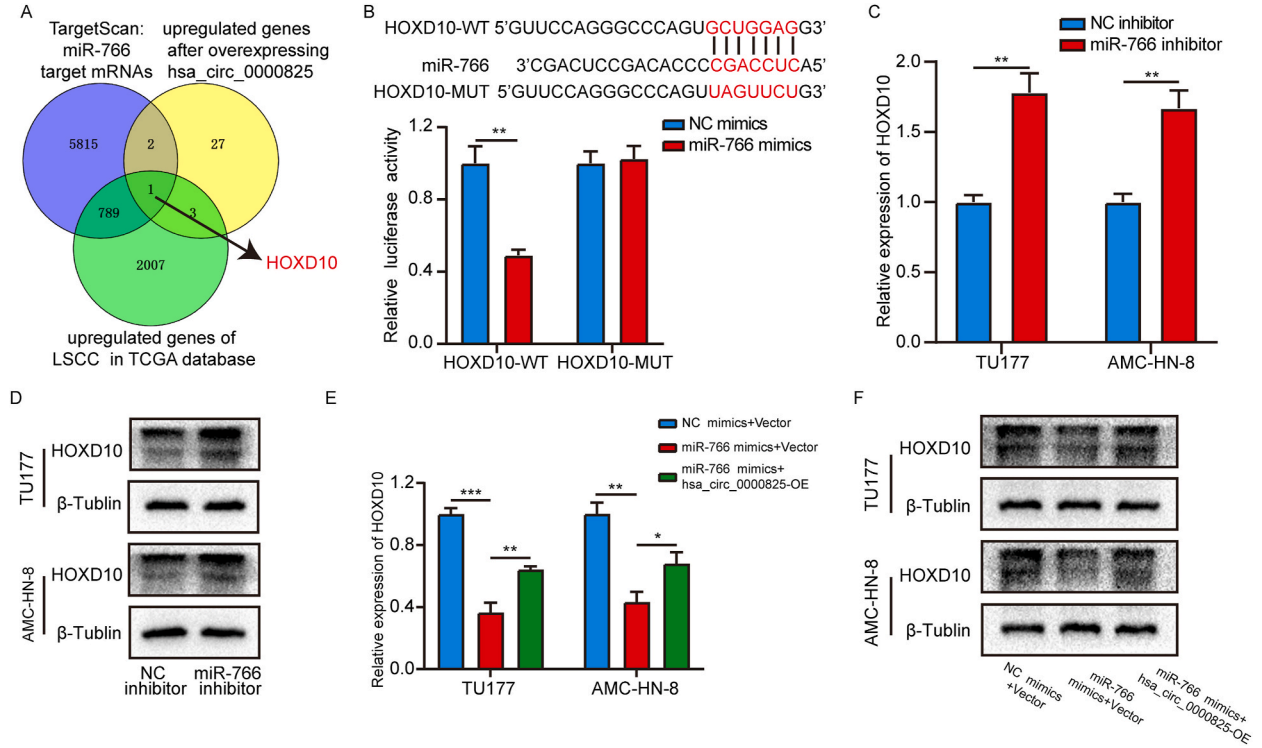


**Fig. 5.** HOXD10 was regulated by hsa_circ_0000825-miR-766 axis in LSCC cells
**A** Combined analysis to screen for miR-766-binding mRNAs. **B** The miR-766 mimics and wild type (HOXD10-WT) or mutant (HOXD10-MUT) HOXD10-luciferase reporter vector were co-transfected into HEK293T cells, and the luciferase activity was detected. **C&D** The effect of miR-766 on HOXD10 was verified by qRT-PCR and Western blot analysis. **E&F** qRT-PCR and Western blot analysis demonstrated that hsa_circ_0000825 could attenuate the influence of miR-766 mimics on HOXD10 expression in LSCC cells. $^{*}P < 0.05$, $^{**}P < 0.01$, $^{***}P < 0.001$.

on the luciferase activity of the hsa_circ_0000825 mutant reporter gene (Fig. 3D).

### *3.5. MiR-766 partially mediates the pro-oncogenic function of hsa_circ_0000825 in LSCC*

We further performed qRT–PCR to detect the expression of miR-766 and found that miR-766 was evidently downregulated in LSCC tissues compared with that in para-cancerous tissues ($P < 0.05$) (Fig. 4A). Next, MTS, colony formation, and transwell assays were conducted to verify the function of miR-766 in TU177 and AMC-HN-8 cells. The results demonstrated that, compared to that observed for the control group, the miR-766 inhibitor distinctly promoted the proliferation, migration, and invasion of TU177 and AMC-HN-8 cells (Fig. 4B–E). Furthermore, the results of the MTS and colony formation assays indicated that the overexpression of hsa_circ_0000825 partially weakened the inhibitory effects of miR-766 mimics on cell viability and proliferation (Fig. 4F and G). Meanwhile, cell migration and invasion were determined using transwell assay. Compared with cells transfected with miR-766 mimics alone, those co-transfected with the hsa_circ_0000825 overexpression plasmid were more capable of migration and invasion (Fig. 4H and I).

### *3.6. HOXD10 is regulated by the hsa_circ_0000825/miR-766 axis in LSCC cells*

To screen the downstream target genes of miR-766, miR-766 target mRNAs from TargetScan, upregulated genes from transcriptomic sequencing in hsa_circ_0000825-overexpressed TU177 cells, and upregulated genes of LSCC in the TCGA database were visually analysed. HOXD10 was not only a miR-766 target mRNA but also an upregulated gene after overexpressing hsa_circ_0000825

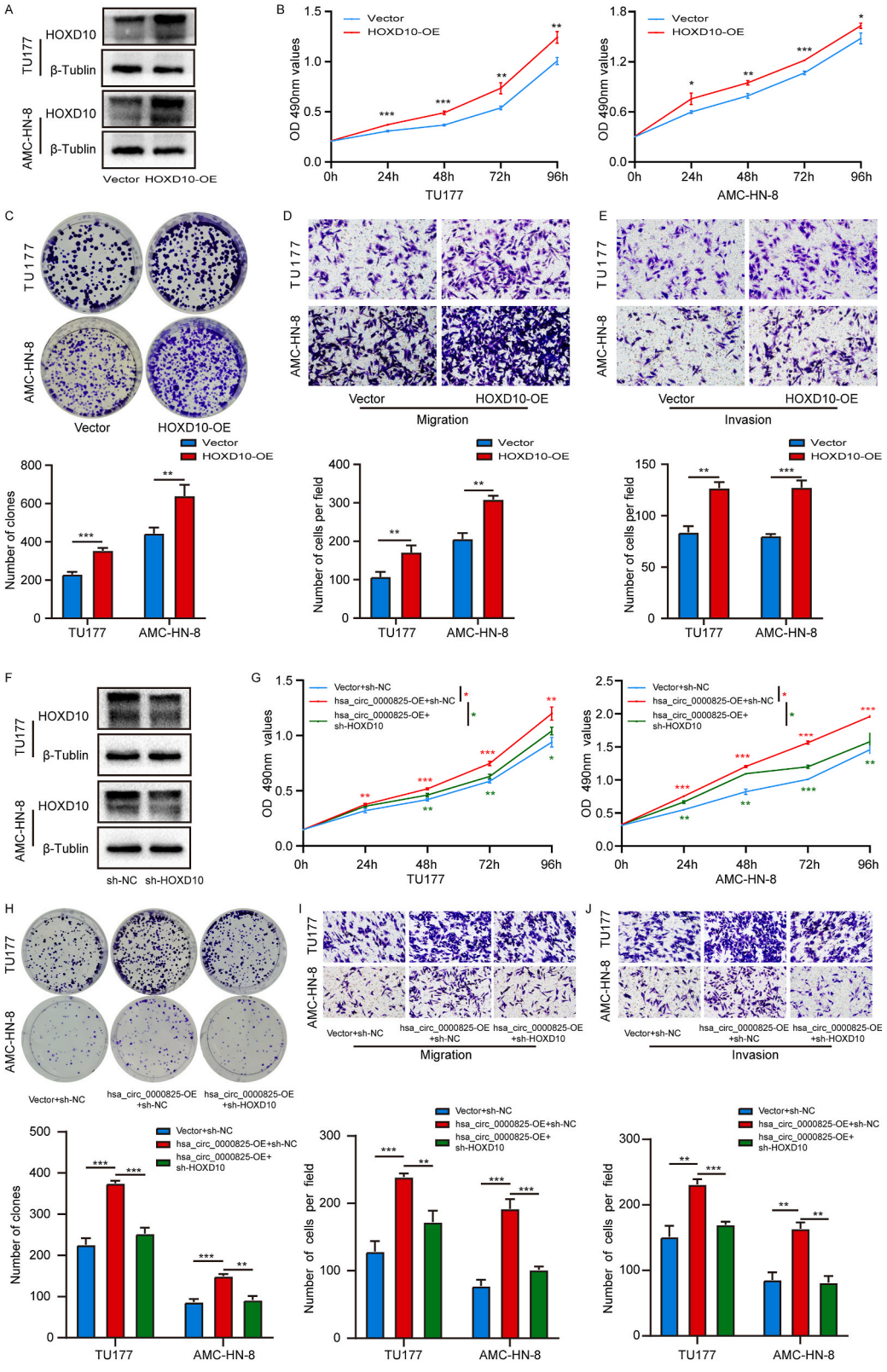


*(caption on next page)*

**Fig. 6.** Downregulation of HOXD10 attenuated the pro-oncogenic effect of hsa_circ_0000825 in LSCC cells
A Western blot analysis was used to verify the successful overexpression of HOXD10 in LSCC cells. **B** The effect of HOXD10 on cell vitality in TU177 and AMC-HN-8 cells was detected by MTS assay. **C** HOXD10 overexpression promoted colony formation of both TU177 and AMC-HN-8 cells. **D&E** The cell migration and invasion ability of TU177 and AMC-HN-8 cells after overexpression of HOXD10 were examined by transwell assay. **F** Western blot analysis was used to verify the successful knockdown of HOXD10 in LSCC cells. **G&H** MTS and colony formation assays indicated that cell proliferation ability of TU177 and AMC-HN-8 cells transfected with overexpression plasmid of hsa_circ_0000825 was reversed when co-transfected with knockdown plasmid of HOXD10. **I&J** Transwell assays demonstrated that cell migration and invasion abilities of TU177 and AMC-HN-8 cells transfected with overexpression plasmid of hsa_circ_0000825 were attenuated when co-transfected with knockdown plasmid of HOXD10. $*P < 0.05$, $**P < 0.01$, $***P < 0.001$.

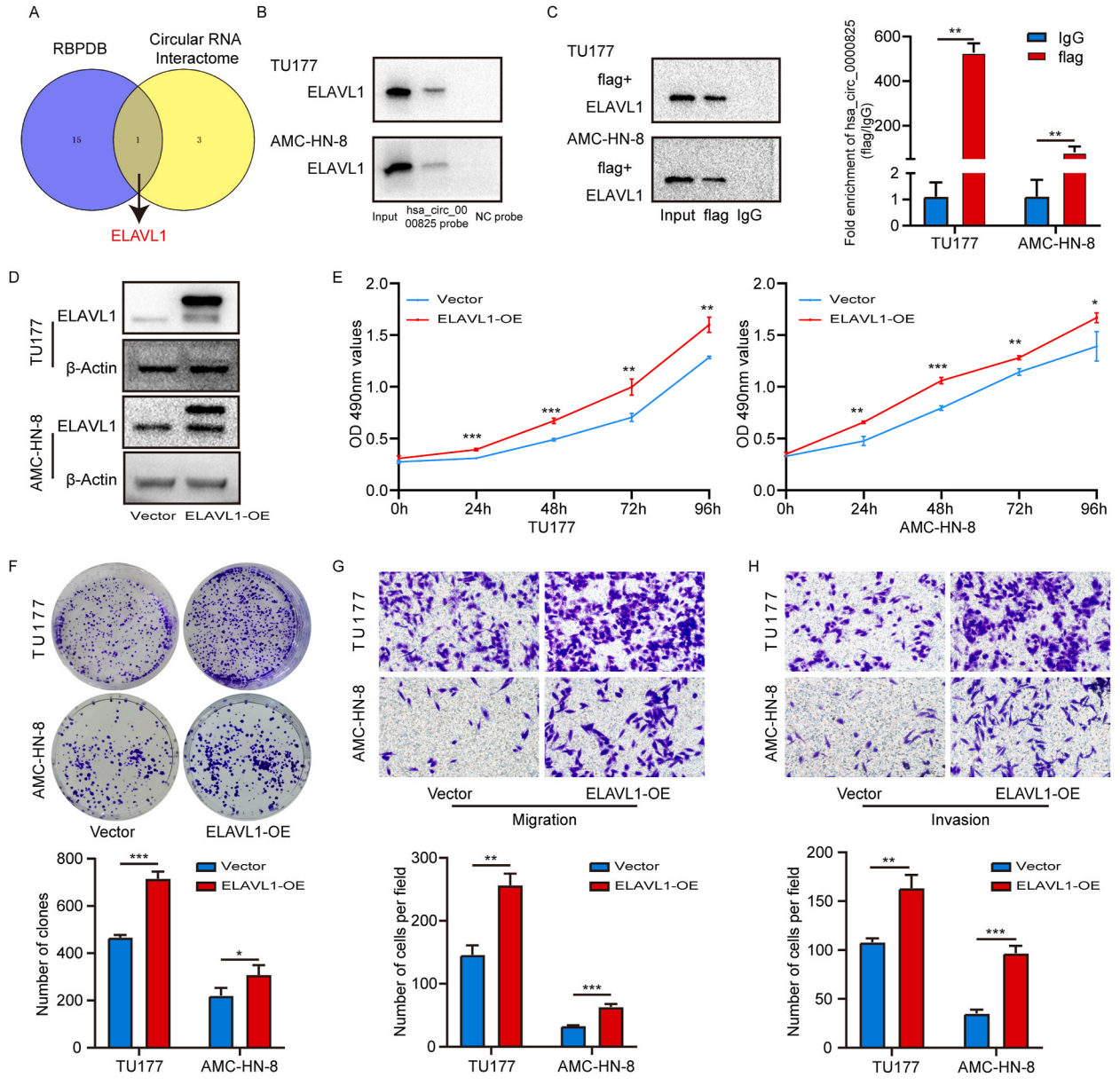


**Fig. 7.** The binding of hsa_circ_0000825 to ELAVL1 was verified, and the function of ELAVL1 in LSCC cells
**A** Combined analysis of two online databases (RBPDB and Circular RNA Interactome) to screen for hsa_circ_0000825-binding proteins. **B&C** Biotinylated-oligo pull-down assay and RIP assay were performed to prove the combination of ELAVL1 and hsa_circ_0000825. **D** Western blot analysis was used to verify the successful overexpression of ELAVL1 in LSCC cells. **E** The effect of ELAVL1 on cell vitality in TU177 and AMC-HN-8 cells was detected by MTS assay. **F** ELAVL1 overexpression promoted colony formation of both TU177 and AMC-HN-8 cells. **G&H** The cell migration and invasion ability of TU177 and AMC-HN-8 cells after overexpression of ELAVL1 were examined by transwell assay. $*P < 0.05$, $**P < 0.01$, $***P < 0.001$.

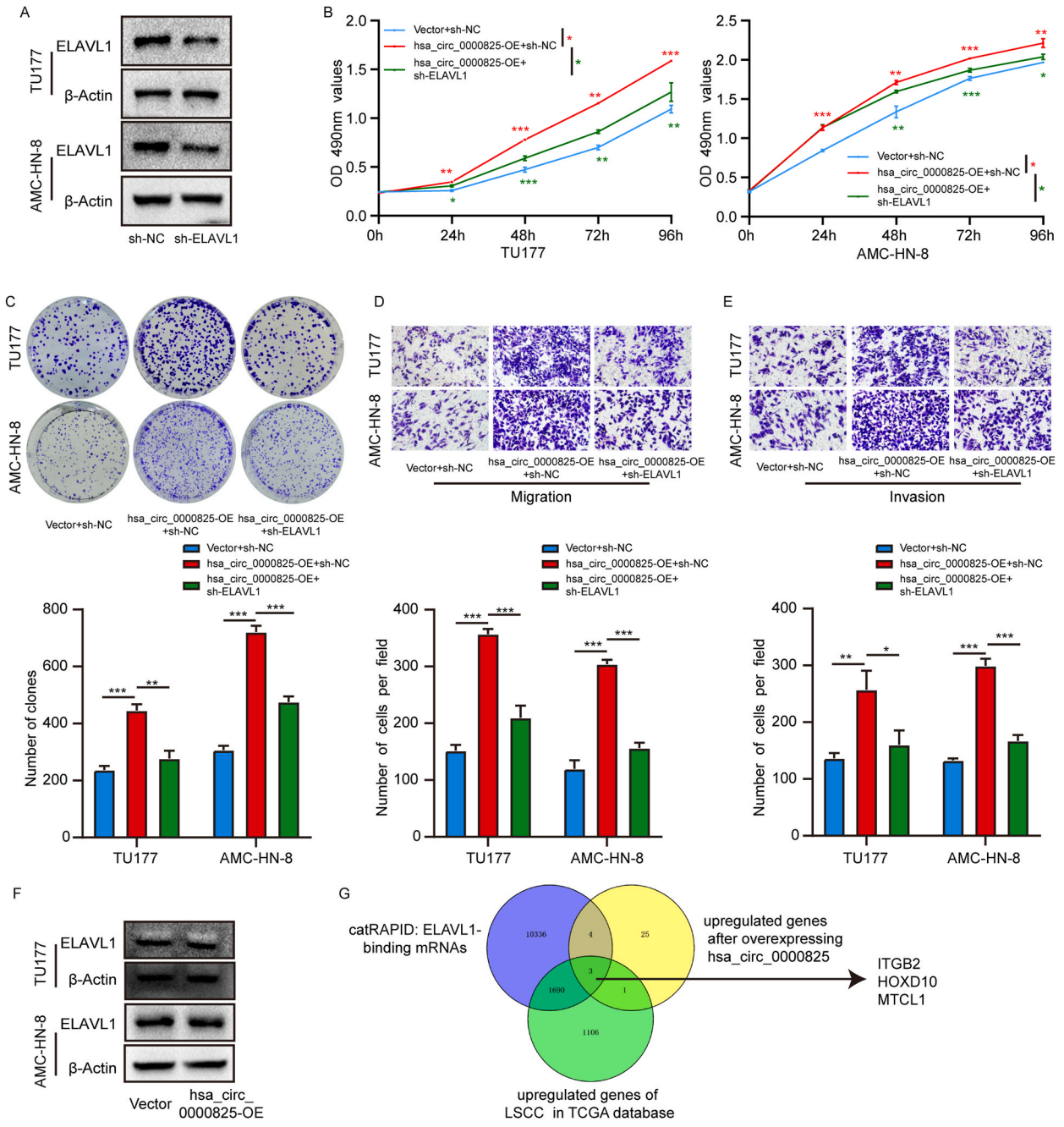


**Fig. 8.** Hsa_circ_0000825 promoted proliferation, migration and invasion of LSCC cells via ELAVL1
**A** Western blot analysis was used to verify the successful knockdown of ELAVL1 in LSCC cells. **B&C** MTS and colony formation assays indicated that cell proliferation ability of TU177 and AMC-HN-8 cells transfected with overexpression plasmid of hsa_circ_0000825 was partially reversed when co-transfected with knockdown plasmid of ELAVL1. **D&E** Transwell assays demonstrated that cell migration and invasion abilities of TU177 and AMC-HN-8 cells transfected with overexpression plasmid of hsa_circ_0000825 were attenuated when co-transfected with knockdown plasmid of ELAVL1. **F** Western blot analysis was performed to detect the effect of hsa_circ_0000825 on ELAVL1 expression. **G** Combined analysis to screen for ELAVL1-binding mRNAs. $*P < 0.05$, $**P < 0.01$, $***P < 0.001$.

and an upregulated gene of LSCC (Fig. 5A). Next, dual-luciferase reporter assay was performed to confirm the direct binding of HOXD10 3′UTR and miR-766. The results revealed that miR-766 mimics decreased the luciferase activity of the wild-type reporter gene by approximately 51 % but not that of the mutant reporter gene ($P < 0.01$) (Fig. 5B). Furthermore, the expression of HOXD10 at the mRNA and protein levels increased significantly after transfection with the miR-766 inhibitor compared to that in the negative control group (Fig. 5C and D). In addition, qRT-PCR analysis demonstrated that HOXD10 mRNA expression was reduced by approximately 63

% and 57 % in TU177 and AMC-HN-8 cells transfected with miR-766 mimics, respectively, relative to control cells. Subsequently, the overexpression of hsa_circ_0000825 caused nearly 1.75-fold and 1.57-fold increases in HOXD10 mRNA expression in miR-766 mimics-transfected TU177 and AMC-HN-8 cells, respectively (Fig. 5E). Similarly, Western blot analysis confirmed that HOXD10 protein level decreased in TU177 and AMC-HN-8 cells transfected with miR-766 mimics compared to those in control cells, and overexpression of hsa_circ_0000825 significantly increased HOXD10 protein level in miR-766 mimics-transfected TU177 and AMC-HN-8 cells (Fig. 5F).

### 3.7. Downregulation of HOXD10 attenuates the pro-oncogenic effect of hsa_circ_0000825 in LSCC cells

To further investigate whether HOXD10 is involved in the pro-oncogenic effects of hsa_circ_0000825, we initially transfected HOXD10 overexpression plasmid into TU177 and AMC-HN-8 cells. As shown in Fig. 6A, the transfection effectively increased the protein level of HOXD10. Subsequently, we conducted cellular functional detection, including MTS, colony formation, and transwell assays, to explore the direct effect of HOXD10 on cells. MTS assay revealed that the overexpression of HOXD10 greatly enhanced the viability of TU177 and AMC-HN-8 cells (Fig. 6B). The colony formation assay demonstrated that the upregulation of HOXD10 resulted in an increase in cell proliferation of approximately 1.54 times and 1.44 times in TU177 and AMC-HN-8 cells, respectively (Fig. 6C). The transwell assay results showed that the migration of TU177 and AMC-HN-8 cells in HOXD10 upregulated group was increased by approximately 1.6 times and 1.5 times, respectively (Fig. 6D). Similarly, the overexpression of HOXD10 significantly promoted the invasion of TU177 and AMC-HN-8 cells (Fig. 6E).

Next, we conducted rescue experiments in TU177 and AMC-HN-8 cells co-transfected with the hsa_circ_0000825 recombinant expression plasmid and HOXD10 shRNA to investigate the functional connection between hsa_circ_0000825 and HOXD10. As shown in Fig. 6F, the HOXD10 shRNA successfully reduced the protein levels of HOXD10. The MTS assay indicated that the downregulation of HOXD10 partially counteracted the enhanced effects of hsa_circ_0000825 overexpression on LSCC cells viability (Fig. 6G). Moreover, HOXD10 knockdown decreased the proliferation of hsa_circ_0000825-overexpressed TU177 and AMC-HN-8 cells by approximately 33 % and 39 %, respectively (Fig. 6H). Meanwhile, the migration ability of overexpressed hsa_circ_0000825 TU177 and AMC-HN-8 cells transfected with HOXD10 shRNA decreased by approximately 28 % and 47 %, respectively, compared with overexpressed hsa_circ_0000825 cells transfected with the pGenesil-1 empty vector (Fig. 6I). Similarly, the transwell assay showed that the invasion ability of cells overexpressing hsa_circ_0000825 transfected with HOXD10 shRNA was evidently decreased compared with the cells transfected with only the hsa_circ_0000825 recombinant expression plasmid (Fig. 6J).

### 3.8. Hsa_circ_0000825 promotes proliferation, migration, and invasion of LSCC cells by binding to ELAVL1

CircRNAs not only act as miRNA sponges but also function by binding to RBPs. To predict hsa_circ_0000825 associated RBPs, two databases (RBPDB and Circular RNA Interactome) were used. ELAVL1 was revealed to be a putative binding RBP of hsa_circ_0000825 (Fig. 7A). Subsequently, we performed pull-down assay using biotinylated oligo probe targeting hsa_circ_0000825 back-spliced sequence. The results showed that ELAVL1 was enriched in the hsa_circ_0000825 probe group but not in the negative control group (Figs. 3C & 7B). In addition, we transfected 3xFLAG-tagged ELAVL1 overexpression plasmid into TU177 and AMC-HN-8 cells and conducted RIP assay using FLAG antibody. The enrichment of hsa_circ_0000825 in the FLAG antibody group was significantly higher than that in the IgG group (Fig. 7C), suggesting that hsa_circ_0000825 binds to ELAVL1.

To explore the potential involvement of ELAVL1 in the pro-oncogenic effects of hsa_circ_0000825, we initially transfected an overexpression plasmid of ELAVL1 into TU177 and AMC-HN-8 cells. As shown in Fig. 7D, transfection successfully increased the protein level of ELAVL1. Next, we performed cellular functional detection, including MTS, colony formation, and transwell assays, to investigate the direct effect of ELAVL1 on LSCC cells. MTS assay demonstrated that the overexpression of ELAVL1 significantly increased the viability of TU177 and AMC-HN-8 cells (Fig. 7E). Colony formation assay showed that the up-regulation of ELAVL1 led to a respective increase in cell proliferation of approximately 1.53 times and 1.40 times in TU177 and AMC-HN-8 cells (Fig. 7F). The results of the transwell assay indicated that the migration of TU177 and AMC-HN-8 cells in the ELAVL1-upregulated group was enhanced by approximately 1.76 times and 1.92 times, respectively (Fig. 7G). Similarly, the overexpression of ELAVL1 significantly promoted the invasion of TU177 and AMC-HN-8 cells (Fig. 7H).

Subsequently, we performed rescue experiments in TU177 and AMC-HN-8 cells co-transfected with the hsa_circ_0000825 overexpression plasmid and ELAVL1 shRNA to examine the functional relationship between hsa_circ_0000825 and ELAVL1. As shown in Fig. 8A, ELAVL1 shRNA effectively decreased the protein level of ELAVL1. The MTS assay revealed that reducing the expression of ELAVL1 partially mitigated the intensified effects of hsa_circ_0000825 overexpression on the viability of LSCC cells (Fig. 8B). Moreover, ELAVL1 knockdown decreased cell proliferation by approximately 38 % and 34 % in hsa_circ_0000825-overexpressed TU177 and AMC-HN-8 cells, respectively (Fig. 8C). Meanwhile, the migration ability of overexpressed hsa_circ_0000825 TU177 and AMC-HN-8 cells transfected with ELAVL1 shRNA decreased by approximately 41 % and 49 %, respectively, compared to that of overexpressed hsa_circ_0000825 cells transfected with pGenesil-1 empty vector (Fig. 8D). Consistently, ELAVL1 depletion greatly reversed the promoting effect of hsa_circ_0000825 overexpression on TU177 and AMC-HN-8 cells invasion (Fig. 8E).

CircRNAs can interact with RBPs and modulate their stability. To further study the exact mechanism by which hsa_circ_0000825/ELAVL1 regulates LSCC progression, we first determined the effect of hsa_circ_0000825 on ELAVL1 using Western blot analysis. However, there was no significant change in the protein levels of ELAVL1 after overexpression of hsa_circ_0000825 (Fig. 8F). We further reviewed the literature and found that ELAVL1 could regulate the stability and translation efficiency of target mRNA by specifically binding to mediate the development and progression of various tumours. To screen the downstream target mRNAs of ELAVL1, ELAVL1-binding mRNAs from catRAPID, upregulated genes from transcriptomic sequencing in hsa_circ_0000825-

overexpressed TU177 cells, along with upregulated genes of LSCC in TCGA database, were visually analysed. The results indicate that ITGB2, HOXD10, and MTCL1 may be crucial downstream target mRNAs of ELAVL1 in LSCC, participating in the pro-oncogenic effect of the hsa_circ_0000825/ELAVL1 axis (Fig. 8G).

## 4. Discussion

Increasing numbers of circRNAs have been proven to be differentially expressed in LSCC, which can promote or inhibit the progression of LSCC. [15] In this study, we found that hsa_circ_0000825 was highly expressed in LSCC tissues. Furthermore, high hsa_circ_0000825 expression was positively associated with advanced clinical stages, lymph node metastasis, and poor survival. Inconsistent with our results, Tang et al. revealed that the expression of hsa_circ_0000825 in colorectal cancer tissues is significantly lower than that in para-carcinoma tissues [16]. These suggest that circRNAs exhibit tissue-specific expression patterns. [17] In the further functional study, overexpression of hsa_circ_0000825 promoted the proliferation, migration, and invasion of LSCC cells *in vitro* and the growth of xenograft tumours derived from TU177 cells *in vivo*. Similarly, Wang et al. showed that hsa_circ_0000825 may be involved in the development of Hirschsprung's disease by influencing cell migration and proliferation. [18].

The competitive endogenous RNA (ceRNA) hypothesis proposes that transcripts such as circRNAs and lncRNAs, which have the same miRNA-binding site as that of mRNA, affect the stability or translation of target mRNAs by competitively binding to miRNAs [19]. In the present study, we confirmed that hsa_circ_0000825 was mainly located in the cytoplasm of LSCC cells. The AGO2-RIP assay revealed that hsa_circ_0000825 was significantly enriched in AGO2-precipitated complexes of LSCC cells. AGO2 is the catalytic component of the RNA-induced silencing complex and is important for miRNA-mediated gene silencing [20]. Therefore, we suspected that hsa_circ_0000825 may function as a miRNA sponge. Previous studies have shown that hsa_circ_0000825 may function as a miR-145-5p sponge to regulate the expression of SMAD3 in Hirschsprung's disease [18]. In this study, direct binding between hsa_circ_0000825 and miR-766 was confirmed through bioinformatics analysis, biotinylated-oligo pull-down assay, and dual-luciferase reporter assay. After exploring the expression of miR-766 in our own specimen library via qRT-PCR, miR-766 was downregulated in LSCC tissues compared to that in para-carcinoma tissues, implying that miR-766 may act as a tumour suppressor. In addition, the miR-766 inhibitor promoted the proliferation, migration, and invasion of LSCC cells. Similarly, miR-766 has been reported as a tumour suppressor gene that influences the malignant progression of colorectal cancer [21] and papillary thyroid carcinoma [22]. However, Zhang et al. revealed that miR-766 inhibition suppressed cutaneous squamous cell carcinoma cell proliferation, metastasis, and glycolysis [23]. Subsequent rescue assays indicated that the overexpression of hsa_circ_0000825 partially reversed the miR-766 mimics-inhibited proliferation, migration, and invasion of TU177 and AMC-HN-8 cells, suggesting that miR-766 partially mediates the pro-oncogenic effect of hsa_circ_0000825. Previous studies have shown that miR-766 partially mediates the pro-oncogenic effects of circ_0021093 in hepatocellular carcinoma [24]. In addition, a series of experiments verified that miR-766 could bind to the HOXD10 3′UTR and influence the expression of HOXD10 at mRNA and protein levels. Furthermore, the overexpression of hsa_circ_0000825 attenuated the inhibitory effect of miR-766 mimics on HOXD10. Similarly, Liu et al. have shown that circPCNXL2 can regulate the expression of SRSF1 by sponging miR-766 in intrahepatic cholangiocarcinoma [25]. HOXD10 is a member of the Abd-B homeobox family and encodes a protein with a homeobox DNA-binding domain [26]. Hakami et al. revealed that HOXD10 overexpression increased cell proliferation, adhesion, and migration but decreased cell invasion in head and neck squamous cell carcinoma [27]. In addition, it was reported that HOXD10 promoted cell proliferation and migration of LSCC [28]. In this study, the results of MTS, colony formation, and transwell assays demonstrated the oncogenic effects of HOXD10 in LSCC. HOXD10 knockdown weakened the promoting effect of hsa_circ_0000825 overexpression on the proliferation, migration, and invasion of TU177 and AMC-HN-8 cells. Therefore, we confirmed that the competitive binding of hsa_circ_0000825 and miR-766 relieved the inhibition of HOXD10 expression by miR-766, upregulated the expression of HOXD10, and further promoted the proliferation, migration, and invasion of LSCC cells.

CircRNAs not only act as miRNA sponges but also function by binding to RBPs [29]. To identify hsa_circ_0000825-binding RBPs, bioinformatics analysis was performed, and the results showed that ELAVL1, also known as HuR, is a putative binding partner of hsa_circ_0000825. Next, using biotinylated-oligo pull-down and RIP assays, the binding between hsa_circ_0000825 and ELAVL1 was confirmed. Cho et al. revealed that the expression of HuR in LSCC tissues was significantly higher than that in normal and dysplastic laryngeal epithelium [30]. Chen et al. reported that circRHOBTB3 bound to HuR to repress metastasis in colorectal cancer [31]. Additionally, it is reported that circDLC1 regulated liver cancer progression via interaction with HuR [32]. In this study, ELAVL1 knockdown attenuated the promoting effect of hsa_circ_0000825 overexpression on the proliferation, migration, and invasion of TU177 and AMC-HN-8 cells. Based on these results, we confirmed that hsa_circ_0000825 could bind to ELAVL1 and play a pro-oncogenic role in LSCC. Furthermore, to study the exact mechanism by which hsa_circ_0000825/ELAVL1 regulates the progression of LSCC, we first determined the effect of hsa_circ_0000825 on ELAVL1 using Western blot analysis. However, hsa_circ_0000825 did not affect the protein levels of ELAVL1 in TU177 or AMC-HN-8 cells. It is reported that HuR regulates the stability and translation efficiency of target mRNA by specifically binding to mediate the development and progression of various tumours [33]. Several oncogenic circRNAs have been reported to promote the stability of target mRNAs by interacting with HuR. For example, He et al. showed that circATG7 acted as a scaffold to increase the interaction between HuR protein and ATG7 mRNA, thereby enhancing ATG7 mRNA stability in pancreatic cancer [34]. Zhu et al. showed that circTICRR interacted with HuR protein, thereby stabilizing GLUD1 mRNA in cervical cancer [35]. Moreover, it is reported that circTHBS1 could enhance the HuR-mediated mRNA stability of INHBA, thereby activating TGF-β pathway and promoting gastric cancer progression [36]. In the present study, to screen the downstream target mRNAs of ELAVL1, ELAVL1-binding mRNAs from catRAPID, upregulated genes from transcriptomic sequencing in hsa_circ_0000825-overexpressed TU177 cells, and upregulated genes of LSCC in TCGA database were visually analysed. The results suggested that ITGB2, HOXD10, and MTCL1 might be crucial downstream target mRNAs of ELAVL1 in LSCC, participating in the

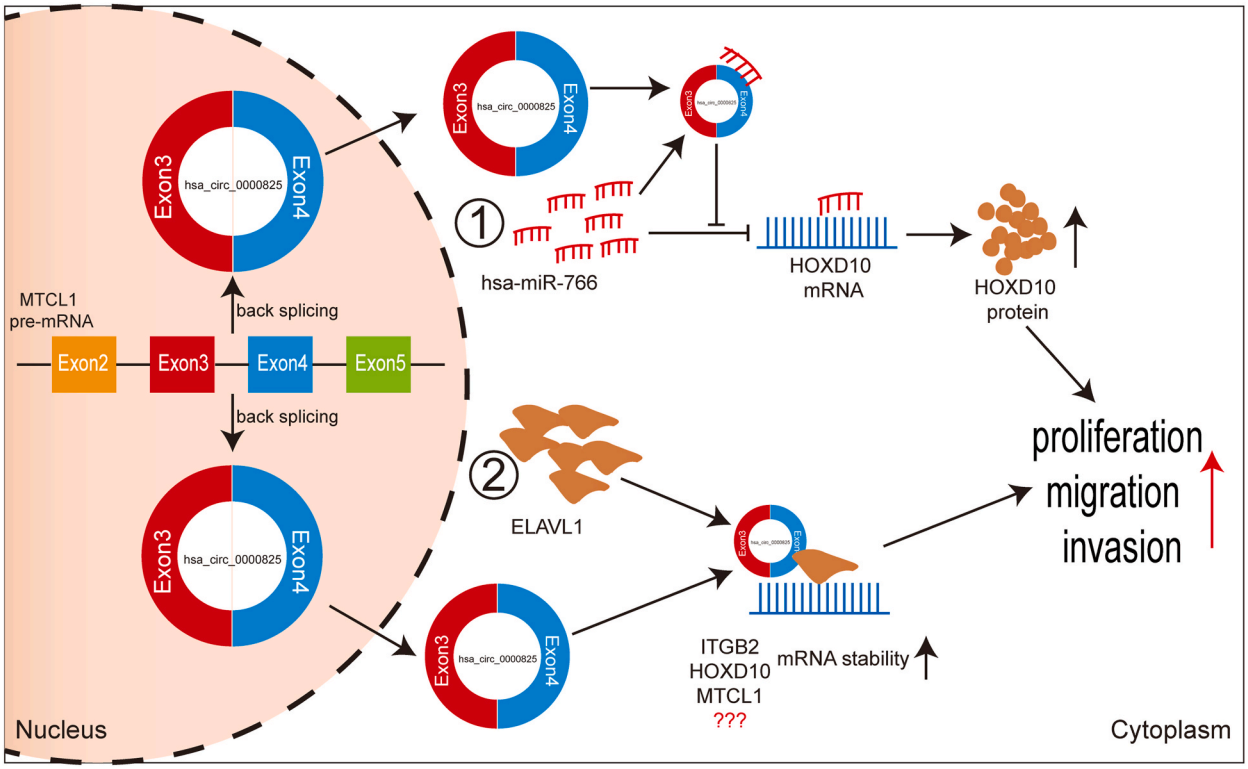


**Fig. 9.** Schematic illustration of the proposed mechanism of hsa_circ_0000825 in LSCC.

pro-oncogenic effects of the hsa_circ_0000825/ELAVL1 axis. However, currently, only bioinformatics analysis and RNA-sequencing data support this result. In future research, a series of *in vitro* and *in vivo* experiments need to be carried out to fully confirm this hypothesis.

## 5. Conclusion

Overall, this study indicates that hsa_circ_0000825 plays a pro-oncogenic role in LSCC via the miR-766/HOXD10 axis and ELAVL1 (Fig. 9) and may be a promising specific biomarker and therapeutic target for laryngeal squamous cell carcinoma.

## Ethics approval and consent to participate

Human tissue study was approved by Medical Ethics Committee of Hebei Medical University (P2022067, March 10, 2022). And all enrolled patients signed written informed consent forms. Animal experiments of this study were approved by Laboratory Animal Ethical and Welfare Committee of Hebei Medical University (LACUC-Hebmu-P 2022101, March 11, 2022).

## Funding

This research is supported by the Natural Science Foundation of Hebei Province (grant number H2022206376), the S&T Program of Hebei (grant number 20577716D), and the Medical Science Research Project Plan Project of Hebei Province Health Commission (grant number 20221139).

## Data availability statement

Data will be made available on request.

## CRediT authorship contribution statement

**Miaomiao Yu:** Writing – original draft, Investigation, Formal analysis, Data curation, Conceptualization. **Huan Cao:** Methodology, Investigation, Data curation, Funding acquisition. **Jianwang Yang:** Methodology, Investigation. **Tao Liu:** Methodology, Investigation. **Baoshan Wang:** Writing – review & editing, Supervision, Funding acquisition, Conceptualization.

## Declaration of competing interest

The authors declare that they have no known competing financial interests or personal relationships that could have appeared to influence the work reported in this paper.

## Appendix A. Supplementary data

Supplementary data to this article can be found online at https://doi.org/10.1016/j.heliyon.2024.e37264.

## References


[1] M. Falco, C. Tammaro, T. Takeuchi, A.M. Cossu, G. Scafuro, S. Zappavigna, A. Itro, R. Addeo, M. Scrima, A. Lombardi, F. Ricciardiello, C. Irace, M. Caraglia, G. Misso, Overview on molecular biomarkers for laryngeal cancer: looking for New answers to an old problem, Cancers 14 (7) (2022), https://doi.org/10.3390/cancers14071716.

[2] H. Sung, J. Ferlay, R.L. Siegel, M. Laversanne, I. Soerjomataram, A. Jemal, F. Bray, Global cancer statistics 2020: GLOBOCAN estimates of incidence and mortality worldwide for 36 cancers in 185 countries, CA A Cancer J. Clin. 71 (3) (2021) 209–249, https://doi.org/10.3322/caac.21660.

[3] C.E. Steuer, M. El-Deiry, J.R. Parks, K.A. Higgins, N.F. Saba, An update on larynx cancer, CA A Cancer J. Clin. 67 (1) (2017) 31–50, https://doi.org/10.3322/caac.21386.

[4] W. Gao, C. Zhang, W. Li, H. Li, J. Sang, Q. Zhao, Y. Bo, H. Luo, X. Zheng, Y. Lu, Y. Shi, D. Yang, R. Zhang, Z. Li, J. Cui, Y. Zhang, M. Niu, J. Li, Z. Wu, H. Guo, C. Xiang, J. Wang, J. Hou, L. Zhang, R.F. Thorne, Y. Cui, Y. Wu, S. Wen, B. Wang, Promoter methylation-regulated miR-145-5p inhibits laryngeal squamous cell carcinoma progression by targeting FSCN1, Mol. Ther. : the Journal of the American Society of Gene Therapy 27 (2) (2019) 365–379, https://doi.org/10.1016/j.ymthe.2018.09.018.

[5] M.L. Ludwig, A.C. Birkeland, R. Hoesli, P. Swiecicki, M.E. Spector, J.C. Brenner, Changing the paradigm: the potential for targeted therapy in laryngeal squamous cell carcinoma, Cancer Biology & Medicine 13 (1) (2016), https://doi.org/10.28092/j.issn.2095-3941.2016.0010.

[6] Cancer of the larynx—cancer stat facts. https://seer.cancer.gov/statfacts/html/laryn.html. (Accessed 26 September 2023).

[7] S. Meng, H. Zhou, Z. Feng, Z. Xu, Y. Tang, P. Li, M. Wu, CircRNA: functions and properties of a novel potential biomarker for cancer, Mol. Cancer 16 (1) (2017) 94, https://doi.org/10.1186/s12943-017-0663-2.

[8] Y. Zhong, Y. Du, X. Yang, Y. Mo, C. Fan, F. Xiong, D. Ren, X. Ye, C. Li, Y. Wang, F. Wei, C. Guo, X. Wu, X. Li, Y. Li, G. Li, Z. Zeng, W. Xiong, Circular RNAs function as ceRNAs to regulate and control human cancer progression, Mol. Cancer 17 (1) (2018) 79, https://doi.org/10.1186/s12943-018-0827-8.

[9] L.S. Kristensen, T. Jakobsen, H. Hager, J. Kjems, The emerging roles of circRNAs in cancer and oncology, Nat. Rev. Clin. Oncol. 19 (3) (2022) 188–206, https://doi.org/10.1038/s41571-021-00585-y.

[10] B. Han, J. Chao, H. Yao, Circular RNA and its mechanisms in disease: from the bench to the clinic, Pharmacol. Ther. 187 (2018) 31–44, https://doi.org/10.1016/j.pharmthera.2018.01.010.

[11] F. Wang, Y. Niu, K. Chen, X. Yuan, Y. Qin, F. Zheng, Z. Cui, W. Lu, Y. Wu, D. Xia, Extracellular vesicle-packaged circATP2B4 mediates M2 macrophage polarization via miR-532-3p/SREBF1 Axis to promote epithelial ovarian cancer metastasis, Cancer Immunol. Res. 11 (2) (2023) 199–216, https://doi.org/10.1158/2326-6066.CIR-22-0410.

[12] M. Chen, B. Tian, G. Hu, Y. Guo, METTL3-Modulated circUHRF2 promotes colorectal cancer stemness and metastasis through increasing DDX27 mRNA stability by recruiting IGF2BP1, Cancers 15 (12) (2023), https://doi.org/10.3390/cancers15123148.

[13] S. Chen, K. Li, J. Guo, H.-N. Chen, Y. Ming, Y. Jin, F. Xu, T. Zhang, Y. Yang, Z. Ye, W. Liu, H. Ma, J. Cheng, J.-K. Zhou, Z. Li, S. Shen, L. Dai, Z.-G. Zhou, H. Xu, Y. Peng, circNEIL3 inhibits tumor metastasis through recruiting the E3 ubiquitin ligase Nedd4L to degrade YBX1, Proceedings of the National Academy of Sciences of the United States of America 120 (13) (2023) e2215132120, https://doi.org/10.1073/pnas.2215132120.

[14] R. Song, S. Ma, J. Xu, X. Ren, P. Guo, H. Liu, P. Li, F. Yin, M. Liu, Q. Wang, L. Yu, J. Liu, B. Duan, N.A. Rahman, S. Wołczyński, G. Li, X. Li, A novel polypeptide encoded by the circular RNA ZKSCAN1 suppresses HCC via degradation of mTOR, Mol. Cancer 22 (1) (2023) 16, https://doi.org/10.1186/s12943-023-01719-9.

[15] S. Wu, X. Huang, X. Tie, Y. Cheng, X. Xue, M. Fan, Role and mechanism of action of circular RNA and laryngeal cancer, Pathol. Res. Pract. 223 (2021) 153460, https://doi.org/10.1016/j.prp.2021.153460.

[16] J. Tang, Low Expression of Hsa_circ_0000825 in Colorectal Cancer and its Clinical Significance, Guangxi Medical University, 2019.

[17] Y. Zhang, Z. Tian, H. Ye, X. Sun, H. Zhang, Y. Sun, Y. Mao, Z. Yang, M. Li, Emerging functions of circular RNA in the regulation of adipocyte metabolism and obesity, Cell Death Discov 8 (1) (2022) 268, https://doi.org/10.1038/s41420-022-01062-w.

[18] C. Wang, C. Luo, Y. Yang, X. Hou, N. Li, J. Yang, H. Yang, K. Wu, L. Yang, Circular RNA MTCL1 targets SMAD3 by sponging miR-145-5p for regulation of cell proliferation and migration in Hirschsprung's disease, Pediatr. Surg. Int. 40 (1) (2023) 25, https://doi.org/10.1007/s00383-023-05621-9.

[19] D.W. Thomson, M.E. Dinger, Endogenous microRNA sponges: evidence and controversy, Nat. Rev. Genet. 17 (5) (2016) 272–283, https://doi.org/10.1038/nrg.2016.20.

[20] K.-W. Min, M.H. Jo, S. Shin, S. Davila, R.W. Zealy, S.I. Kang, L.T. Lloyd, S. Hohng, J.-H. Yoon, AUF1 facilitates microRNA-mediated gene silencing, Nucleic Acids Res. 45 (10) (2017) 6064–6073, https://doi.org/10.1093/nar/gkx149.

[21] X.-X. He, S.-S. Luo, H.-Q. Qin, X.-W. Mo, MicroRNA-766-3p-mediated downregulation of HNF4G inhibits proliferation in colorectal cancer cells through the PI3K/AKT pathway, Cancer Gene Ther. 29 (6) (2022) 803–813, https://doi.org/10.1038/s41417-021-00362-0.

[22] Z. Li, J. Xu, H. Guan, J. Lai, X. Yang, J. Ma, Circ_0059354 aggravates the progression of papillary thyroid carcinoma by elevating ARFGEF1 through sponging miR-766-3p, J. Endocrinol. Invest. 45 (4) (2022) 825–836, https://doi.org/10.1007/s40618-021-01713-2.

[23] Z. Zhang, H. Sun, J. Hou, L. Li, L. Wu, Circular RNA circFADS2 inhibits the progression of cutaneous squamous cell carcinoma by regulating miR-766-3p/HOXA9 axis, Histol. Histopathol. 37 (4) (2022) 335–348, https://doi.org/10.14670/HH-18-409.

[24] L. Liu, X. Qi, Y. Gui, H. Huo, X. Yang, L. Yang, Overexpression of circ_0021093 circular RNA forecasts an unfavorable prognosis and facilitates cell progression by targeting the miR-766-3p/MTA3 pathway in hepatocellular carcinoma, Gene 25 (2019) 143992, https://doi.org/10.1016/j.gene.2019.143992.

[25] S. Liu, Y. Wang, T. Wang, K. Shi, S. Fan, C. Li, R. Chen, J. Wang, W. Jiang, Y. Zhang, Y. Chen, X. Xu, Y. Yu, C. Li, X. Li, CircPCNXL2 promotes tumor growth and metastasis by interacting with STRAP to regulate ERK signaling in intrahepatic cholangiocarcinoma, Mol. Cancer 23 (1) (2024) 35, https://doi.org/10.1186/s12943-024-01950-y.

[26] J. Zákány, M. Kmita, D. Duboule, A dual role for Hox genes in limb anterior-posterior asymmetry, Science (New York, N.Y.) 304 (5677) (2004) 1669–1672, https://doi.org/10.1126/science.1096049.

[27] F. Hakami, L. Darda, P. Stafford, P. Woll, D.W. Lambert, K.D. Hunter, The roles of HOXD10 in the development and progression of head and neck squamous cell carcinoma (HNSCC), Br. J. Cancer 111 (4) (2014) 807–816, https://doi.org/10.1038/bjc.2014.372.

[28] R. de Barros E Lima Bueno, A. Ramão, D.G. Pinheiro, C.P. Alves, V. Kannen, A.A. Jungbluth, L.F. de Araújo, B.R. Muys, A.S. Fonseca, J.R. Plaça, R.A. Panepucci, L. Neder, F.P. Saggioro, R.C.M. Mamede, D.L.A. Figueiredo, W.A. Silva, HOX genes: potential candidates for the progression of laryngeal squamous cell carcinoma, Tumour Biol 37 (11) (2016) 15087–15096, https://doi.org/10.1007/s13277-016-5356-8.

[29] Z.-H. Zhang, Y. Wang, Y. Zhang, S.-F. Zheng, T. Feng, X. Tian, M. Abudurexiti, Z.-D. Wang, W.-K. Zhu, J.-Q. Su, H.-L. Zhang, G.-H. Shi, Z.-L. Wang, D.-L. Cao, D.-W. Ye, The function and mechanisms of action of circular RNAs in Urologic Cancer, Mol. Cancer 22 (1) (2023) 61, https://doi.org/10.1186/s12943-023-01766-2.
[30] N.-P. Cho, H.-S. Han, Y. Soh, K.-Y. Lee, H.-J. Son, Cytoplasmic HuR over-expression is associated with increased cyclooxygenase-2 expression in laryngeal squamous cell carcinomas, Pathology 39 (6) (2007) 545–550, https://doi.org/10.1080/00313020701684391.
[31] J. Chen, Y. Wu, X. Luo, D. Jin, W. Zhou, Z. Ju, D. Wang, Q. Meng, H. Wang, X. Fu, J. Xu, Z. Song, Circular RNA circRHOBTB3 represses metastasis by regulating the HuR-mediated mRNA stability of PTBP1 in colorectal cancer, Theranostics 11 (15) (2021) 7507–7526, https://doi.org/10.7150/thno.59546.
[32] H. Liu, T. Lan, H. Li, L. Xu, X. Chen, H. Liao, X. Chen, J. Du, Y. Cai, J. Wang, X. Li, J. Huang, K. Yuan, Y. Zeng, Circular RNA circDLC1 inhibits MMP1-mediated liver cancer progression via interaction with HuR, Theranostics 11 (3) (2021) 1396–1411, https://doi.org/10.7150/thno.53227.
[33] X. Wu, L. Xu, The RNA-binding protein HuR in human cancer: a friend or foe? Adv. Drug Deliv. Rev. 184 (2022) 114179 https://doi.org/10.1016/j.addr.2022.114179.
[34] Z. He, K. Cai, Z. Zeng, S. Lei, W. Cao, X. Li, Autophagy-associated circRNA circATG7 facilitates autophagy and promotes pancreatic cancer progression, Cell Death Dis. 13 (3) (2022) 233, https://doi.org/10.1038/s41419-022-04677-0.
[35] T. Zhu, Y. Cen, Z. Chen, Y. Zhang, L. Zhao, J. Wang, W. Lu, X. Xie, X. Wang, Oncogenic circTICRR suppresses autophagy via binding to HuR protein and stabilizing GLUD1 mRNA in cervical cancer, Cell Death Dis. 13 (5) (2022) 479, https://doi.org/10.1038/s41419-022-04943-1.
[36] S. Qiu, B. Li, Y. Xia, Z. Xuan, Z. Li, L. Xie, C. Gu, J. Lv, C. Lu, T. Jiang, L. Fang, P. Xu, J. Yang, Y. Li, Z. Chen, L. Zhang, L. Wang, D. Zhang, H. Xu, W. Wang, Z. Xu, CircTHBS1 drives gastric cancer progression by increasing INHBA mRNA expression and stability in a ceRNA- and RBP-dependent manner, Cell Death Dis. 13 (3) (2022) 266, https://doi.org/10.1038/s41419-022-04720-0.